



Title	Three-dimensional imaging of a long-period stacking ordered phase in $\text{Mg}_{97}\text{Zn}_1\text{Gd}_2$ using high-voltage electron microscopy
Author(s)	Sato, Kazuhisa; Tashiro, Shunya; Yamaguchi, Yohei et al.
Citation	Materials Transactions. 2016, 57(6), p. 918-921
Version Type	VoR
URL	<a href="https://hdl.handle.net/11094/89449">https://hdl.handle.net/11094/89449</a>
rights	
Note	

*The University of Osaka Institutional Knowledge Archive : OUKA*

<https://ir.library.osaka-u.ac.jp/>

The University of Osaka

# Three-Dimensional Imaging of a Long-Period Stacking Ordered Phase in $\text{Mg}_{97}\text{Zn}_1\text{Gd}_2$ Using High-Voltage Electron Microscopy

Kazuhisa Sato<sup>1,2,\*</sup>, Shunya Tashiro<sup>3</sup>, Yohei Yamaguchi<sup>3</sup>, Takanori Kiguchi<sup>1</sup>, Toyohiko J. Konno<sup>1</sup>, Tomokazu Yamamoto<sup>4</sup>, Kazuhiro Yasuda<sup>4</sup> and Syo Matsumura<sup>4</sup>

<sup>1</sup>Institute for Materials Research, Tohoku University, Sendai 980–8577, Japan

<sup>2</sup>Present Address: Research Center for Ultra-High Voltage Electron Microscopy, Osaka University, Ibaraki 567–0047, Japan

<sup>3</sup>Department of Materials Science, Tohoku University, Sendai 980–8579, Japan

<sup>4</sup>Department of Applied Quantum Physics and Nuclear Engineering, Kyushu University, Fukuoka 812–8581, Japan

Spatial configurations and lateral morphology of the 14H long-period stacking ordered (LPSO) phase have been studied by single tilt-axis electron tomography using high-voltage scanning transmission electron microscopy (STEM) operated at 1 MV. A “Quonset hut-like” lateral shape of the LPSO was found in a tomogram of a specimen as thick as 1.7  $\mu\text{m}$ . The reconstructed volume reveals spatial distribution of residual particulate precipitates of  $(\text{Mg}, \text{Zn})_3\text{Gd}$  phase 20–30 nm in diameters. The precipitates act as a source of solute elements for the formation and growth processes of 14H LPSO. 1 MV-STEM realizes enough resolution for imaging the morphology of LPSO as well as high electron transmittance ( $\sim 4.1 \mu\text{m}$ ) without any obvious electron irradiation damages on microstructures. [doi:10.2320/matertrans.M2016021]

(Received January 19, 2016; Accepted March 15, 2016; Published April 15, 2016)

**Keywords:** high-voltage electron microscopy (HVEM), long-period stacking order (LPSO), magnesium-zinc-gadolinium, electron tomography, lateral growth, scanning transmission electron microscopy (STEM)

## 1. Introduction

Magnesium alloys containing transition metal (TM) together with rare earth (RE) elements, such as Mg–Zn–Y, have been attracting much interest as next generation lightweight structural materials. The mechanical strength of the materials can be attributed to the characteristic long-period stacking order (LPSO) (synchronized LPSO) formed in the  $\alpha$ -Mg matrix<sup>1)</sup>. Recent extensive studies based on scanning transmission electron microscopy (STEM)<sup>2–4)</sup> revealed atomic structures of the LPSO; however, the images obtained by this technique are projections of three-dimensional (3D) objects. To overcome this fundamental limitation, we have studied 3D shapes and spatial distribution of LPSO by electron tomography using a 300 kV-STEM<sup>5)</sup>. As a result, it was turned out that the lateral growth of LPSO parallel to the  $(0001)_{\text{Mg}}$  is so fast that the overall in-plane shape of the LPSO cannot be imaged by using the conventional STEM regarding electron transmittance. To better understand the nature of the formation behavior of the LPSO, we hence intend to characterize 3D structures of the LPSO using high-voltage transmission electron microscopy (HVEM). According to the literature, the maximum observable limit for electrons accelerated at 1 MV is as thick as 15  $\mu\text{m}$  for Al<sup>6)</sup> and 8  $\mu\text{m}$  for Si<sup>7)</sup>. Recently, Sadamatsu *et al.* succeeded in imaging dislocations in Si as thick as 10  $\mu\text{m}$  using HVEM equipped with an in-column type energy filter<sup>8)</sup>. Thus, HVEM is a promising technique to visualize interior structures of a thick specimen. The purpose of this study is to analyze lateral shapes and spatial distribution of the LPSO formed in  $\text{Mg}_{97}\text{Zn}_1\text{Gd}_2$  alloys by means of single-axis tilt tomography using HVEM. It should be mentioned that key issue here is not only electron transmittance but also resolution enough to image microstructures of fine precipitates.

## 2. Experimental Procedure

The Mg–Zn–Gd cast alloy ingots were prepared using high-frequency induction heating in an Ar atmosphere. The nominal composition of the alloy is  $\text{Mg}_{97}\text{Zn}_1\text{Gd}_2$  (at%). The as-cast alloys were annealed at 773 K in an Ar atmosphere for 0.06 and 18 ks, and then quenched into ice water. To prepare samples for TEM, disk-shaped specimens were mechanically thinned followed by Ar ion milling. Details of the TEM specimen preparation can be found in the literature<sup>5)</sup>. Microstructures of the alloy were characterized using an FEI TITAN<sup>3</sup> 60–300 STEM operating at 300 kV. Elemental analyses were performed using energy dispersive x-ray spectroscopy (EDX) attached to the STEM. We used a JEOL JEM-1300NEF HVEM for electron tomography. Tilt-series of high-angle annular dark-field (HAADF) STEM images were obtained at 1 MV. Based on a prior careful inspection of contrast, images were sequentially recorded from 0° to –66° and then 0° to 60° with the tilt axis increment of 2°. To ensure field of view at high tilt angles, additional images were obtained at 61°, 63° and 65°. Thus, totally 67 images were acquired. We employed a weighted back-projection method for 3D reconstruction of the obtained tilt-series dataset after tilt-axis alignment using a software (System in Frontier, Composer).

## 3. Results and Discussion

Figure 1(a) shows a HAADF-STEM image and a selected area electron diffraction (SAED) pattern of a specimen after aging at 773 K for 0.06 ks. The SAED pattern was obtained from the  $\alpha$ -Mg matrix with beam incidence parallel to  $[\bar{1}2\bar{1}0]_{\text{Mg}}$ . A large precipitate lying across the field of view from the top right corner to bottom left is the  $(\text{Mg}, \text{Zn})_3\text{Gd}$ -type secondary phase<sup>9)</sup>, which exists in an as-cast alloy. It is noted that the precipitate is highly enriched in solute elements of Zn and Gd, in contrast to the  $\alpha$ -Mg matrix. Fine bright

\*Corresponding author, E-mail: sato@uhvem.osaka-u.ac.jp

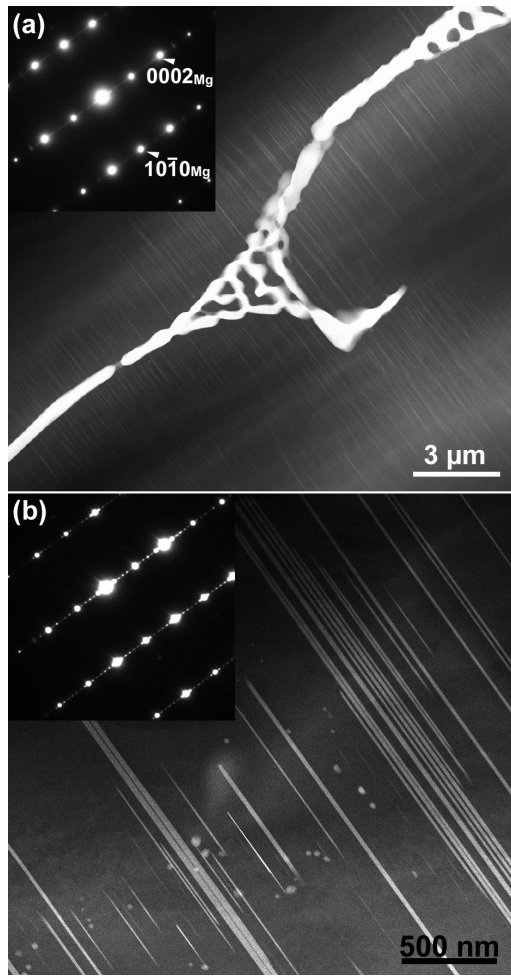


Fig. 1 (a) HAADF-STEM image and SAED pattern of a  $\text{Mg}_{97}\text{Zn}_1\text{Gd}_2$  cast alloy after aging at 773 K for 0.06 ks. (b) HAADF-STEM image and SAED pattern of a  $\text{Mg}_{97}\text{Zn}_1\text{Gd}_2$  cast alloy after aging at 773 K for 18 ks. Both images were obtained with beam incidence parallel to  $[\bar{1}2\bar{1}0]_{\text{Mg}}$ .

straight lines seen around the precipitate are solute-segregated stacking faults (SFs)<sup>8)</sup>, which appear as atomic number (Z) contrasts. Correspondingly, electron diffraction shows weak streaks in the  $[0001]^*_{\text{Mg}}$  direction. Such a dense solute-segregated SFs are always observed in adjacent to  $(\text{Mg}, \text{Zn})_3\text{Gd}$  precipitates. A prolonged aging at 773 K leads to the formation of 14H-type LPSO and shrinkage of  $(\text{Mg}, \text{Zn})_3\text{Gd}$  precipitates. Figure 1(b) shows a HAADF-STEM image and an SAED pattern of a specimen after aging at 773 K for 18 ks. The beam incidence is in the  $[\bar{1}2\bar{1}0]_{\text{Mg}}$  direction. Appearance of six satellite reflections indicates the formation of 14H LPSO, which is clearly seen as bright straight bands/lines in the HAADF-STEM image. Small particulate precipitates dispersed in addition to the LPSO are the shrunk secondary phase remained in the matrix. To clearly visualize 3D distribution of LPSO and the residual precipitates, we performed electron tomography using 1 MV-STEM.

Figure 2 shows HAADF-STEM images of the 14H LPSO taken from a tilt-series dataset obtained at 1 MV. The tilt angles are as follows: (a)  $0^\circ$ , (b)  $50^\circ$ , and (c)  $-50^\circ$ . Tilt axis is in the vertical direction in the images. Figure 2(a) was observed with the beam incidence of  $[\bar{1}2\bar{1}0]_{\text{Mg}}$ . The distribution of LPSO is clearly seen as bright straight bands/lines with

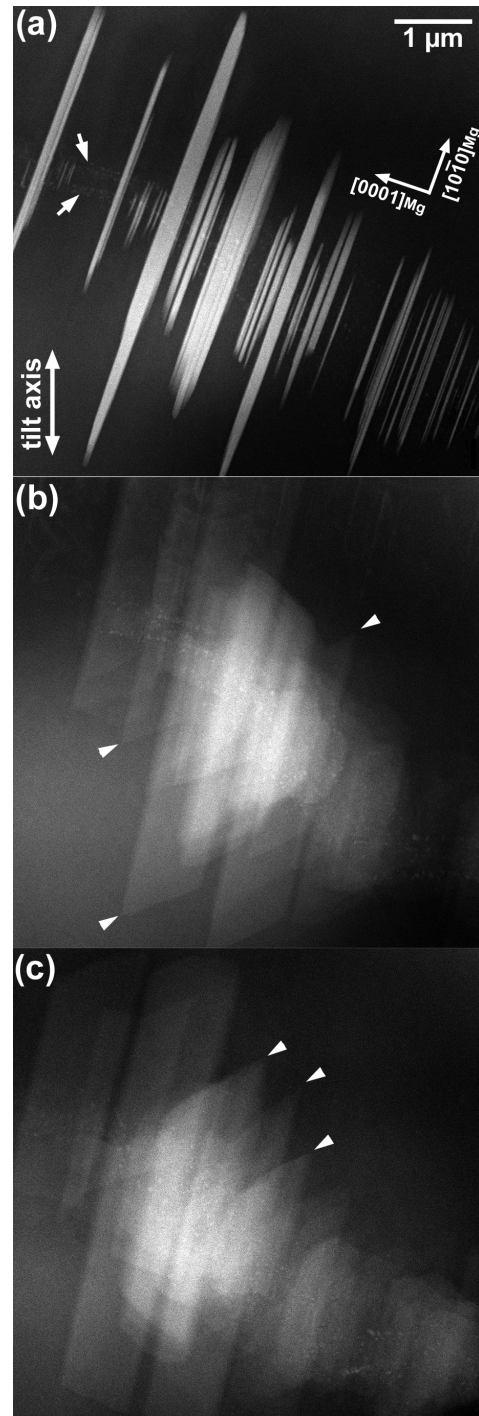


Fig. 2 Snapshots of HAADF-STEM images depicted from a tilt series observed at 1 MV for a specimen after aging at 773 K for 18 ks. (a) The beam incidence is parallel to  $[\bar{1}2\bar{1}0]_{\text{Mg}}$ . (b) Tilt angle of  $50^\circ$ . (c) Tilt angle of  $-50^\circ$ .

thickness of around 50 nm in the  $[0001]_{\text{Mg}}$  direction (some of them reached  $\sim 200$  nm in thick). Arrows indicate residual precipitates 20–30 nm in sizes. Images obtained at high tilt angle of  $\pm 50^\circ$  give lateral structural information of the LPSO. As seen in Figs. 2(b) and 2(c), edges of the LPSO show a characteristic triangular shape as indicated by arrowheads. The foil thickness of the observed area was estimated to be as thick as  $1.7 \mu\text{m}$ , which was deduced by  $t / \cos(50^\circ)$  where  $t$  denotes the lateral width of LPSO band measured in Fig. 2(b). It should be mentioned that at the maximum tilt angle of  $66^\circ$



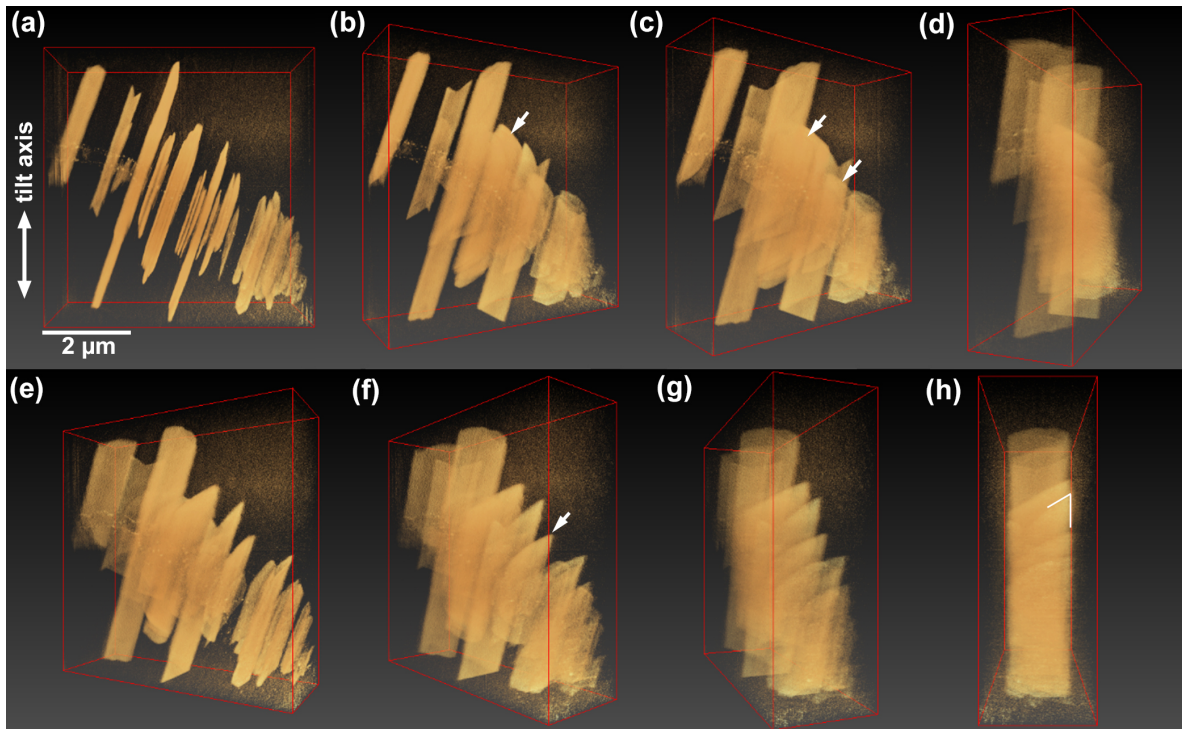


Fig. 3 Reconstructed 3D volumes of a  $\text{Mg}_{97}\text{Zn}_1\text{Gd}_2$  cast alloy after aging at 773 K for 18 ks. The reconstructed volume is  $5665 \text{ nm} \times 5857 \text{ nm} \times 1989 \text{ nm}$  with the pixel size of 5.8 nm/pixel. The foil thickness is  $\sim 1700 \text{ nm}$ . Tilt angle with respect to the original tilt axis is as follows: (a)  $0^\circ$ , (b)  $30^\circ$ , (c)  $50^\circ$ , (d)  $70^\circ$ , (e)  $-30^\circ$ , (f)  $-50^\circ$ , (g)  $-70^\circ$ , (h)  $-90^\circ$ .

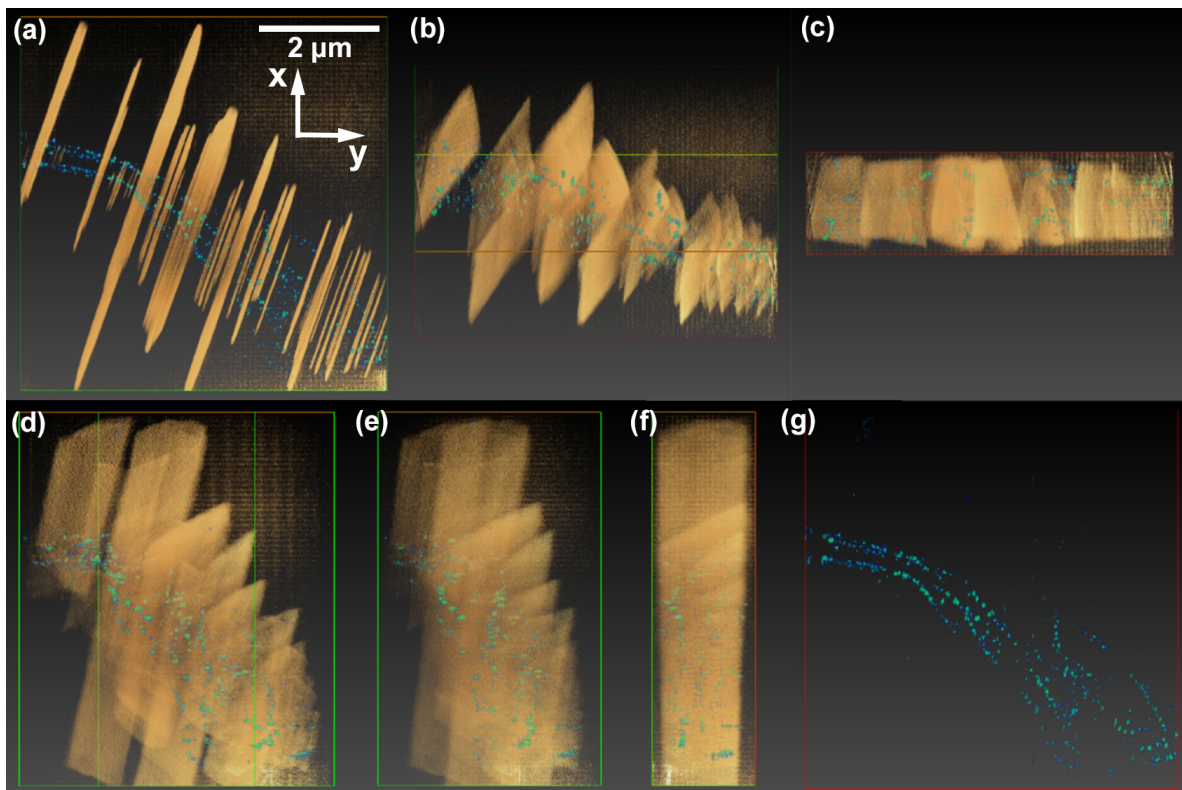


Fig. 4 Reconstructed 3D volumes of a  $\text{Mg}_{97}\text{Zn}_1\text{Gd}_2$  cast alloy after aging at 773 K for 18 ks. Residual particulate precipitates are colored in light blue. Tilt angle with respect to the original tilt axis (x-axis) is as follows: (a)  $0^\circ$ , (b)  $60^\circ$  (tilted around the y-axis), (c)  $90^\circ$  (tilted around the y-axis), (d)  $-50^\circ$ , (e)  $-70^\circ$ , (f)  $-90^\circ$ , (g)  $0^\circ$  (only the precipitates are shown).



the specimen thickness reaches  $4.1\ \mu\text{m}$ ; 1 MV-STEM realizes resolution enough to image 20-nm-sized precipitates as well as high electron transmittance without any obvious electron irradiation damage on microstructures. In general, a raster nature of the STEM and small electron probe with a low current density compared with TEM imaging may prevent severe irradiation damage, but detailed mechanisms are not clear.

Figure 3 shows snapshots of reconstructed 3D images viewed from several directions. The original tilt axis is in the vertical direction of the images. The reconstructed volume is  $5665\ \text{nm} \times 5857\ \text{nm} \times 1989\ \text{nm}$  with the pixel size of  $5.8\ \text{nm}/\text{pixel}$  (specimen thickness is  $\sim 1700\ \text{nm}$ ). As can be seen, 3D configurations of the LPSO are clearly reconstructed. Lateral morphology can be visualized by rotating the reconstructed 3D volume. A “Quonset hut-like” lateral shape of the LPSO is seen in such a thick region as indicated by arrows in Figs. 3(b), 3(c) and 3(f). Such a shape was not observed in our previous study using a 300 kV-STEM for a  $1.2\ \mu\text{m}$ -thick specimen<sup>5)</sup>. Thus, this is a merit of observing a thick specimen. It is noted that edge of each LPSO band has characteristic triangular shapes with edge angle of around  $60^\circ$  with respect to  $(\bar{1}2\bar{1}0)_{\text{Mg}}$  (a typical example is indicated in Fig. 3(h)). In our earlier study<sup>5)</sup>, we found that edge angles distribute between  $30^\circ$  and  $90^\circ$ , with the most frequent appearance of  $\sim 60^\circ$ , which corresponds to a growth front parallel to  $\{11\bar{2}0\}_{\text{Mg}}$ . The present observation for a thicker specimen also confirms that the angle of the most frequent occurrence is  $\sim 60^\circ$ , as previously observed in a thinner specimen<sup>5)</sup>. It is presumed that such a preferable plane for lateral growth of LPSO is related to the in-plane atomic cluster arrangement where the close-packed direction of the  $2\sqrt{3} \times 2\sqrt{3}$  ordered structure is on a line parallel to the original  $\{11\bar{2}0\}_{\text{Mg}}$ <sup>3)</sup>.

To clearly show spatial distribution of the precipitates, small particles are colored in cyan in the reconstructed volume as shown in Fig. 4. As seen, distribution of particulate precipitates, as small as  $\sim 20\ \text{nm}$  in sizes, is not random but rather aligned across approximately central part of each LPSO band. Such a morphology of the precipitates implies that shrink of  $(\text{Mg}, \text{Zn})_3\text{Gd}$  precipitates on aging must be related to the growth of LPSO. Aging time dependence of the volume fraction of the secondary phase has been reported in the literature<sup>10)</sup>. Namely, as the LPSO grows, the secondary phase tends to disappear. STEM-EDX elemental analyses revealed that the secondary phase includes approximately  $\sim 30\ \text{at}\%$  of Zn and Gd. On the other hand, the solute contents in  $\alpha$ -Mg matrix of an as-cast alloy are low as determined by electron probe micro analyzer (Zn:  $0.2\sim 0.3\ \text{at}\%$ , Gd:  $0.5\sim 1.5\ \text{at}\%$ )<sup>11)</sup>. These experimental evidences indicate that  $(\text{Mg}, \text{Zn})_3\text{Gd}$  precipitates act as a source of solute elements for the formation and growth processes of 14H LPSO in  $\text{Mg}_{97}\text{Zn}_1\text{Gd}_2$  alloys, in addition to the solute atoms dissolved in the  $\alpha$ -Mg matrix. According to the latest study on phase diagram of Mg-Zn-Gd alloy<sup>12)</sup>, existence of an invariant reaction,  $\alpha\text{-Mg} + \text{Mg}_3\text{Gd} \rightarrow \text{Mg}_5\text{Gd} + \text{LPSO}$ , has been reported based on experimentally determined isothermal sections at 673 K and 723 K.

## 4. Conclusion

We have studied spatial distribution of 14H LPSO and particulate precipitates of residual  $(\text{Mg}, \text{Zn})_3\text{Gd}$  phase co-exist in an aged  $\text{Mg}_{97}\text{Zn}_1\text{Gd}_2$  cast alloy by means of single tilt-axis electron tomography using 1 MV-STEM. The results can be summarized as follows.

- (1) The foil thickness of the observed area was estimated to be as thick as  $1.7\ \mu\text{m}$ , which reaches  $4.1\ \mu\text{m}$  at the maximum tilt angle of  $66^\circ$ . A “Quonset hut-like” lateral shape of the LPSO was seen in such a thick region.
- (2) 1 MV-STEM realizes enough resolution for imaging the morphology of LPSO as well as high electron transmittance without any obvious electron irradiation damage on microstructures.
- (3) The  $(\text{Mg}, \text{Zn})_3\text{Gd}$  precipitates act as a source of solute elements for the formation and growth processes of 14H LPSO, in addition to the solute atoms dissolved in the  $\alpha$ -Mg matrix.

## Acknowledgments

This study is supported by Grant-in-Aid for Scientific Research on Innovative Areas “Synchro-LPSO” (No. 23109006 & 26109702) from the Ministry of Education, Culture, Sports, Science and Technology, Japan. The authors wish to thank Prof. Y. Kawamura and Dr. M. Yamasaki of Kumamoto University for providing us Mg-Zn-Gd alloys, and Ms. K. Ito for 3D reconstruction. HVEM observation was performed under a support “Research Station for HVEM” Kyushu University. We thank Mr. H. Maeno and Prof. Emeritus Y. Tomokiyo of Kyushu University for their support using the HVEM. KS acknowledges financial support from the Japan Science Technology Agency “Development of systems and technology for advanced measurement and analysis” program and the Tanikawa Fund Promotion of Thermal Technology.

## REFERENCES

- 1) Y. Kawamura, K. Hayashi, A. Inoue and T. Masumoto: *Mater. Trans.* **42** (2001) 1172–1176.
- 2) E. Abe, A. Ono, T. Itoi, M. Yamasaki and Y. Kawamura: *Philos. Mag. Lett.* **91** (2011) 690–696.
- 3) H. Yokobayashi, K. Kishida, H. Inui, M. Yamasaki and Y. Kawamura: *Acta Mater.* **59** (2011) 7287–7299.
- 4) T. Kiguchi, Y. Ninomiya, K. Shimmi, K. Sato and T.J. Konno: *Mater. Trans.* **54** (2013) 668–674.
- 5) K. Sato, S. Matsunaga, S. Tashiro, Y. Yamaguchi, T. Kiguchi and T.J. Konno: *Mater. Trans.* **56** (2015) 928–932.
- 6) H. Fujita and T. Tabata: *Jpn. J. Appl. Phys.* **12** (1973) 471–472.
- 7) G. Thomas and J.-C. Lacaze: *J. Microscopy* **97** (1973) 301–308.
- 8) S. Sadamatsu, M. Tanaka, K. Higashida and S. Matsumura: *Ultramicrosc.* **162** (2016) 10–16.
- 9) M. Yamasaki, M. Sasaki, M. Nishijima, K. Hiraga and Y. Kawamura: *Acta Mater.* **55** (2007) 6798–6805.
- 10) Y. Jono, M. Yamasaki and Y. Kawamura: *Mater. Trans.* **54** (2013) 703–712.
- 11) S. Matsunaga: Master’s Thesis, Tohoku University (2015).
- 12) F. Miyakawa, K. Ikeda, S. Miura, T. Horiuchi and S. Minamoto: Proceedings of the 10<sup>th</sup> International Conference on Magnesium Alloys and Their Applications (2015) 345–349.